Geochemical Perspectives Letters

4.46 Ga zircons anchor chronology of lunar magma ocean

J. Greer, B. Zhang, D. Isheim, D.N. Seidman, A. Bouvier, P.R. Heck

Supplementary Information

The Supplementary Information includes:

- Methods
- Table S-1
- Figures S-1 to S-4
- Supplementary Information References

Methods

The zircon grain Z-14 used in this study measures 22 μm × 12 μm (Fig. 1), and was analysed for U-Pb systematics by Zhang *et al.* (2021) using NanoSIMS. The size of the grain presents some challenges in APT sample preparation. A strong bond to the substrate is essential as the mechanical stresses at the nanotip are large, and a weak point in a sample—such as a grain boundary— can lead to the fracture of a specimen during APT analyses (Kelly and Miller, 2007). A large thick base permits heat introduced by the laser to be more efficiently conducted away from the apex of a nanotip to its base. To avoid the presence of a grain boundary, the nanotips from this zircon need to be shorter than nanotips from larger zircon grains, such as those studied by Valley *et al.* (2014), to be certain that a grain boundary is not included. A lamella of approximately 1 μm × 10 μm was milled with a focused ion beam (FIB) microscope, lifted out (Fig. 1) using a micromanipulator, and subsections of the lamella are firmly attached to Si flat-topped posts with gas injection system (GIS)-deposited Pt. These subsections of the zircon are further milled to produce the nanotips (*e.g.*, Fig. S-1). The material within several nanometres from the surface could have been subjected to sputtering-induced amorphisation during NanoSIMS analyses (Aléon-Toppani *et al.*, 2021). Because of this, the nanotips were fabricated to exclude this zone using the FIB microscope to remove the top material by ion beam milling away the top material. The final FIB microscope sharpening steps are done at a low voltage (5 kV) to minimise the thickness of the damaged/amorphised zone produced by the FIB ion beam. For several of these samples, the APT analyses are significantly larger than the thickness of the amorphised layer (~20 nm), and no differences were noticed between the top of the nanotip that might have been affected by the ion beam and the lower parts of the reconstruction coming from a greater sample depth. Tips D and A2 preserve some of the Pt deposited during sample preparation at the apex.

In atom-probe tomography we apply a high electric field in conjunction with a pulsed picosecond UV laser (λ = 355 nm), which causes field-evaporation and -ionisation of atoms from a nanotip. The field-evaporated ions are then accelerated through a local electrode and detected by a position-sensitive microchannel plate. This method yields both the elemental and isotopic identities and spatial distribution of the atoms in a sample. We used a CAMECA LEAP 5000-

XS equipped with a picosecond UV laser, with a laser pulse energy of 50 or 200 pJ and a pulse repetition rate of 200 kHz. A total of six nanotips were prepared and analysed from zircon Z-14. Tips A, B, and C were located in the righthand NanoSIMS spot (Fig. 1) which yielded a $^{207}Pb/^{206}Pb$ date of 4399 ± 46 Myr, and Tips D, E, F were located in the lefthand NanoSIMS spot which yielded a $^{207}Pb/^{206}Pb$ date of 4453 ± 47 Myr. The first two nanotips (Tips E, F) were unsuccessful, and fractured before steady-state evaporation occurred. These nanotips were analysed with APT conditions (pulse energy of 200 pJ) which had been previously reported for zircon (*e.g.*, Valley *et al.*, 2014), but were unsuitable for these samples. Of the four successful nanotips, all were analysed with a laser pulse energy of 50 pJ. The run for Tip A was stopped manually, then resharpened and reanalysed as Tip A2 (Table S-1). Since resistive materials like zircon can have many different species of complex molecular ions in their mass spectra (*e.g.*, Valley *et al.*, 2015), the conditions for our analyses were chosen to minimise the presence of molecular ions.

Supplementary Tables

Table S-1 Summary of the analytical conditions for APT and yields from the zircon nanotips.

Tip Name	Temperature (K)	Pulse Energy (pJ)	Pulse Rate (kHz)	Total # of detections	Length of tip (nm)
F	50	200	200	n/a	n/a
E	50	200	200	n/a	n/a
D	30	50	200	~14.5 M	~70
C	50	50	200	~7.5 M	~90
B	50	50	200	~18.3 M	~240
A	30	50	200	~31.6 M	~200
A2	30	50	200	~15.0 M	~100

Supplementary Figures

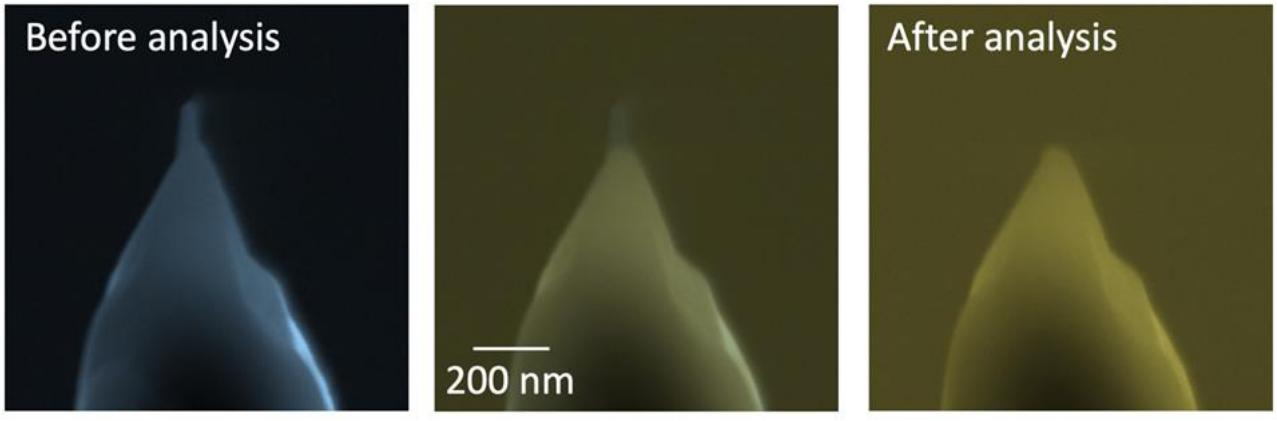

Figure S-1 False-colour SEM images of a Tip A before (left) and after (right) APT analysis, and a composite image in the middle to highlight the amount of material field-evaporated during the APT analysis. After APT analysis, this sample was later re-sharpened to produce Tip A2.

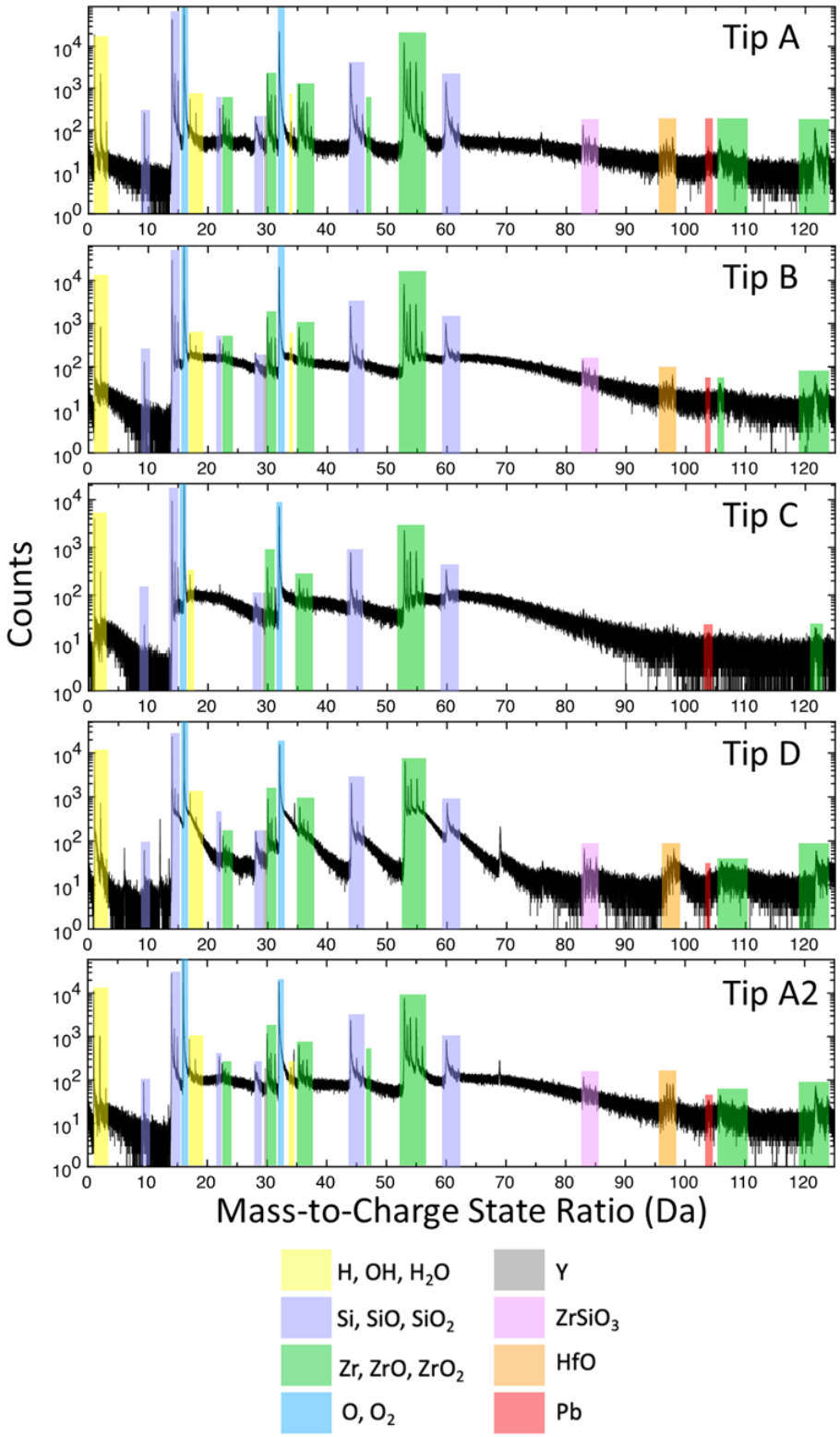

Figure S-2 Mass-to-Charge State Ratio spectra for the 5 nanotips analysed. Important species have been labelled with a corresponding colour. This can include singly, doubly, and triply charged species, as well as complex ions.

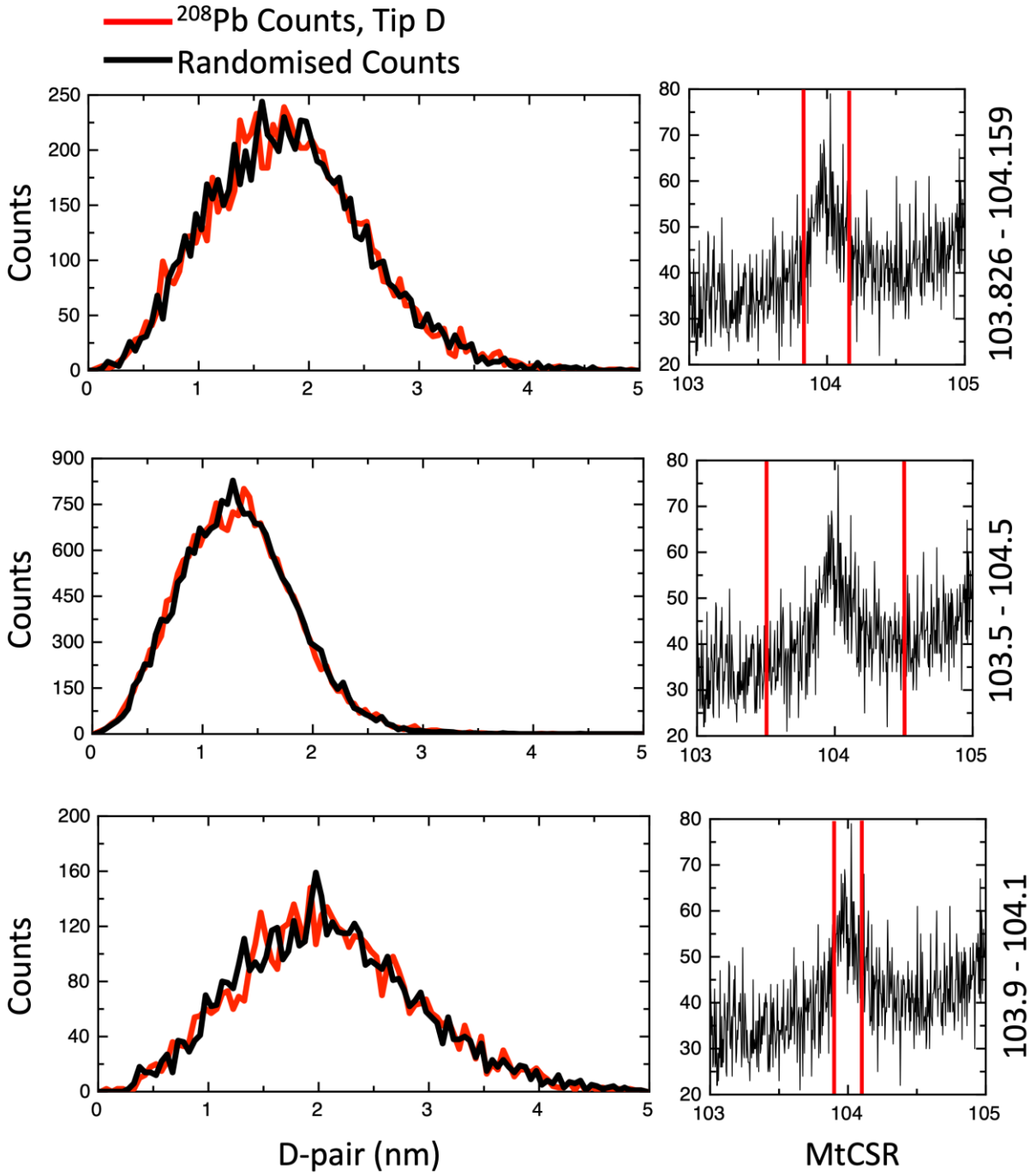

Figure S-3 Nearest neighbour distribution plots with different ranges, showing there is no clustering regardless of how Pb is ranged. The distribution of Pb atoms in the sample (red) and random distribution (black) is plotted to the left. On the right are the mass-to-charge State ratio (MtCSR) spectra showing the range (bracketed by red lines) that was plotted in the left.

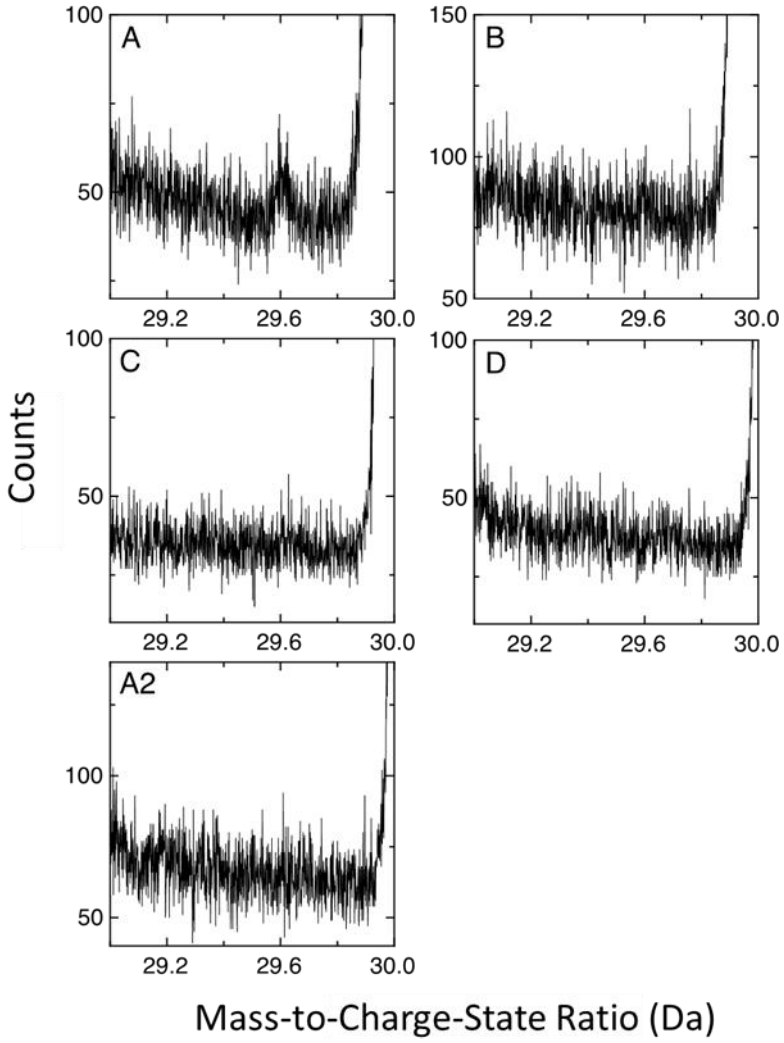

Figure S-4 Mass-to-charge-state ratio spectra for the 5 nanotips analysed between 29 and 30 Da. Only one nanotip, Tip A, shows a peak at 29.67 Da, corresponding to $^{89}Y^{3+}$.

Supplementary Information References

Aléon-Toppani, A., Brunetto, R., Aléon, J., Dionnet, Z., Rubino, S., Levy, D., Troadec, D., Brisset, F., Borondics, F., Brisset, F. (2021) A Preparation Sequence for Multi-Analysis of Micrometer-Sized Extraterrestrial Samples. *Meteoritics and Planetary Science* 56, 1151-1172. https://doi.org/10.1111/maps.13696

Kelly, T.F., Miller, M.K. (2007) Atom probe tomography. *Review of Scientific Instruments* 78, 031101. https://doi.org/10.1063/1.2709758

Valley, J.W., Cavosie, A.J., Ushikubo, T., Reinhard, D.A., Lawrence, D.F., Larson, D.J., Clifton, P.H., Kelly, T.F., Wilde, S.A., Moser, D.E., Spicuzza, M.J. (2014) Hadean age for a post-magma-ocean zircon confirmed by atom-probe tomography. *Nature Geoscience* 7, 219-223. https://doi.org/10.1038/ngeo2075

Valley, J.W., Reinhard, D.A., Cavosie, A.J., Ushikubo, T., Lawrence, D.F., Larson, D.J., Kelly, T.F., Snoeyenbos, D.R., Strickland, A. (2015) Nano-and micro-geochronology in Hadean and Archean zircons by atom-probe tomography and SIMS: New tools for old minerals. *American Mineralogist* 100, 1355-1377. https://doi.org/10.2138/am-2015-5134

Zhang, B., Lin, Y., Moser, D.E., Hao, J., Liu, Y., Zhang, J., Barker, I.R., Li, Q., Shieh, S.R., Bouvier, A. (2021) Radiogenic Pb mobilization induced by shock metamorphism of zircons in the Apollo 72255 Civet Cat norite clast. *Geochimica et Cosmochimica Acta* 302, 175-192. https://doi.org/10.1016/j.gca.2021.03.012